

Manipulation of vortex array via a magnetism-tunable spin-polarized scanning tunnelling microscopy

Bing Xia(夏冰), Hong-Yuan Chen(陈虹源), Jian Zheng(郑健), Bo Yang(杨波), Jie Cai(蔡杰), Yi Zhang(章毅), Yi Yang(杨毅), Hao Yang(杨浩), Dan-Dan Guan(管丹丹), Xiao-Xue Liu(刘晓雪), Liang Liu(刘亮), Yao-Yi Li(李耀义), Shi-Yong Wang(王世勇), Can-Hua Liu(刘灿华), Hao Zheng(郑浩), and Jin-Feng Jia(贾金锋)

Citation: Chin. Phys. B, 2025, 34 (**3**): 037402. DOI: 10.1088/1674-1056/adb38d
Journal homepage: http://cpb.iphy.ac.cn; http://iopscience.iop.org/cpb

What follows is a list of articles you may be interested in

Revisit of the anisotropic vortex states of 2H-$NbSe_2$ towards the zero-field limit

Fan Zhang(张凡), Xingyuan Hou(侯兴元), Yuxuan Jiang(姜宇轩), Zongyuan Zhang(张宗源), Yubing Tu(涂玉兵), Xiangde Zhu(朱相德), Genfu Chen(陈根富), and Lei Shan(单磊)
Chin. Phys. B, 2024, 33 (**6**): 067401. DOI: 10.1088/1674-1056/ad362d

Nonreciprocal transport in the superconducting state of the chiral crystal $NbGe_2$

Yonglai Liu(刘永来), Xitong Xu(许锡童), Miao He(何苗), Haitian Zhao(赵海天), Qingqi Zeng(曾庆祺), Xingyu Yang(杨星宇), Youming Zou(邹优鸣), Haifeng Du(杜海峰), and Zhe Qu(屈哲)
Chin. Phys. B, 2024, 33 (**5**): 057402. DOI: 10.1088/1674-1056/ad334b

Effects of irradiation on superconducting properties of small-grained MgB_2 thin films

Li Liu(刘丽), Jung Min Lee, Yoonseok Han, Jaegu Song, Chorong Kim, Jaekwon Suk, Won Nam Kang, Jie Liu(刘杰), Soon-Gil Jung, and Tuson Park
Chin. Phys. B, 2023, 32 (**12**): 127402. DOI: 10.1088/1674-1056/acf5d3

Role of grain boundary networks in vortex motion in superconducting films

Yu Liu(刘宇), Feng Xue(薛峰), and Xiao-Fan Gou(苟晓凡)
Chin. Phys. B, 2023, 32 (**12**): 127401. DOI: 10.1088/1674-1056/ace315

Experimental observation of pseudogap in a modulation-doped Mott insulator: Sn/Si(111)-($\sqrt{30}\times\sqrt{30}$)*R*30°

Yan-Ling Xiong(熊艳翎), Jia-Qi Guan(关佳其), Rui-Feng Wang(汪瑞峰), Can-Li Song(宋灿立), Xu-Cun Ma(马旭村), and Qi-Kun Xue(薛其坤)
Chin. Phys. B, 2022, 31 (**6**): 067401. DOI: 10.1088/1674-1056/ac65f2

RAPID COMMUNICATION

Manipulation of vortex array via a magnetism-tunable spin-polarized scanning tunnelling microscopy

Bing Xia(夏冰)[1], Hong-Yuan Chen(陈虹源)[1], Jian Zheng(郑健)[1], Bo Yang(杨波)[1], Jie Cai(蔡杰)[1], Yi Zhang(章毅)[1], Yi Yang(杨毅)[1], Hao Yang(杨浩)[1], Dan-Dan Guan(管丹丹)[1], Xiao-Xue Liu(刘晓雪)[1], Liang Liu(刘亮)[1], Yao-Yi Li(李耀义)[1], Shi-Yong Wang(王世勇)[1], Can-Hua Liu(刘灿华)[1], Hao Zheng(郑浩)[1], and Jin-Feng Jia(贾金锋)[1,2,3,†]

[1] *TD Lee Institute, Key Laboratory of Artificial Structures and Quantum Control (Ministry of Education), School of Physics and Astronomy, Shanghai Jiao Tong University, Shanghai* 200240, *China*

[2] *Department of Physics, Southern University of Science and Technology, Shenzhen* 518055, *China*

[3] *Quantum Science Center of Guangdong–Hong Kong–Macao Greater Bay Area (Guangdong), Shenzhen* 518045, *China*

(Received 8 December 2024; revised manuscript received 19 January 2025; accepted manuscript online 7 February 2025)

Manipulating and braiding Majorana zero modes (MZM) are a critical step toward realizing topological quantum computing. The primary challenge is controlling the vortex, which hosts the MZM, within a superconducting film in a spatially precise manner. To address this, we developed a magnetic force-based vortex control technology using the STM system with a self-designed four-electrode piezo-scanner tube and investigated vortex manipulation on the $NbSe_2$ superconducting film. We employed ferromagnetic tips to control the movement of vortex array induced by the tip's remanent magnetism. A magnetic core solenoid device was integrated into the STM system and a strong magnetic tip demagnetization technique was developed, providing a viable technical solution for further enabling single vortex manipulation.

Keywords: vortex manipulation, scanning tunneling microscope, magnetic tip, demagnetization technique

PACS: 74.25.Wx, 75.60.–d, 07.79.Cz, 03.67.Hk

DOI: 10.1088/1674-1056/adb38d **CSTR:** 32038.14.CPB.adb38d

1. Introduction

The scanning tunneling microscope (STM) is a powerful tool for surface physics research. On the one hand, the STM's capability to characterize surface morphology and electronic states has led to the discovery of many novel quantum phenomena in condensed matter physics.[1–10] Among these, the Majorana zero-energy mode (MZM) is of particular interest due to its potential for topological quantum computing in recent years.[5–9] In systems that host the MZM, topological insulator/superconductor heterojunction offers unique advantages, especially the binding of the MZM to Abrikosov vortices, which can be manipulated by moving the position of vortex.[6,7,11,12] On the other hand, an STM is not only a powerful microscope but also able to manipulate single atoms.[13–15] Furthermore, its core component, the scanning head, has been upgraded to a multi-electrode scanning tunneling microscope, providing a foundation for integrating various microscopic characterization and control methods.[16,17]

Braiding of MZMs may provide the strongest evidence for confirming Majorana fermion properties and serves as a key technical pathway for realizing topological quantum computing.[18–20] In theory, MZM braiding schemes have been proposed for both ideal conditions and in practical systems.[21–25] For vortex MZMs, the implementation schemes can be divided into modifications to the instrument and improvements to the sample.[23–25] Various single-vortex manipulation techniques have been realized using scanning probes, including applying magnetic force, thermal effects, mechanical stress and other methods to the vortex in the sample.[26–30] Considering that MZMs are easily destroyed and exist at low temperatures, methods such as pinning the vortex by damaging the sample surface with a tip to create local mechanical stress or inducing vortex rearrangement by locally heating the sample surface to make the superconducting region lose its superconductivity, cannot prevent the destruction of MZMs during the manipulation. In contrast, in magnetic force microscopy (MFM)-based manipulation experiments, where the tip does not touch the sample and the temperature is kept constant, the magnetic manipulation scheme — using the stray magnetic field generated by the magnetic tip to produce a magnetic dipole interaction with the vortex, thereby pulling it to move — has the advantage of protecting MZMs during the moving process.[26,27]

Although magnetically manipulated single-vortex technology is a practical way to control MZMs, it is currently only implemented in MFM. The reason is that MFM detects the magnetic signal rather than the tunneling current and thus can-

†Corresponding author. E-mail: jfjia@sjtu.edu.cn

© 2025 Chinese Physical Society and IOP Publishing Ltd. All rights, including for text and data mining, AI training, and similar technologies, are reserved.

not characterize the electronic properties of MZMs. A feasible solution to address both the measurement and control of MZMs is to improve the experimental approach of MFM's magnetically manipulated vortex technology and integrate it into the STM system. A conventional MFM maintains a constant absolute magnetization of the tip and controls the relative strength of the magnetic force on the vortex by varying the distance between the tip and the sample to manipulate the vortex.[26] However, in STM, the distance between the tip and the sample is fixed at approximately 1 nm, meaning that the relative magnetic strength of the tip on the vortex cannot be altered. Instead, the magnetic force on the vortex can only be adjusted by changing the absolute magnetization of the magnetic tip. To implement this scheme, the simplest method is to wrap a coil around the tip to form a solenoid, applying current to generate a local magnetic field that controls the absolute magnetization of the tip. This approach has been used in spin-polarized scanning tunneling microscopes (Sp-STMs).[31]

Fortunately, the multifunctional scanning tunneling microscope (MSTM) in our lab, equipped with a self-designed four-electrode piezo-scanner tube, provides an opportunity to introduce a similar setup.[16,17] In this paper, we have developed a new technology and demonstrated its capability of vortex control in $NbSe_2$.

2. Methods

The experiments were carried out in a UHV system equipped with a 400 mK STM and MBE. The base pressures of the systems are better than 2×10^{-10} Torr. 2H-$NbSe_2$ crystals were made by the vapor transport method. $NbSe_2$ were cleaved *in situ* at room temperature, resulting in shiny flat (0001) surfaces. After cleavages, $NbSe_2$ samples were immediately transferred to STM head. STM images show atomically flat terraces of several hundreds of nanometers in size. All STM $\mathrm{d}I/\mathrm{d}V$ maps were taken at 400 mK with $V = 1$ mV; $I = 0.1$ nA; $V_{\mathrm{mod}} = 0.05$ mV with a frequency of 991 Hz. The STM tips were made from electrochemically etched metal wires. The solutions to etch W, Fe, Ni, permalloy and FeSiB wires are NaOH, HCl, HCl, HCl and a HCl/HF mixture respectively.

3. Results

Figure 1(a) shows the characterization of a static vortex lattice using a non-magnetic W tip. The image was obtained by $\mathrm{d}I/\mathrm{d}V$ measurement at around 1 mV, i.e., the coherence peak of $NbSe_2$. In the image, high-intensity (red) regions correspond to the superconducting areas, while low-intensity (blue) regions correspond to the vortices. Based on the image, we know that vortex lattice has a spacing of 167 nm under 0.1 T magnetic field.

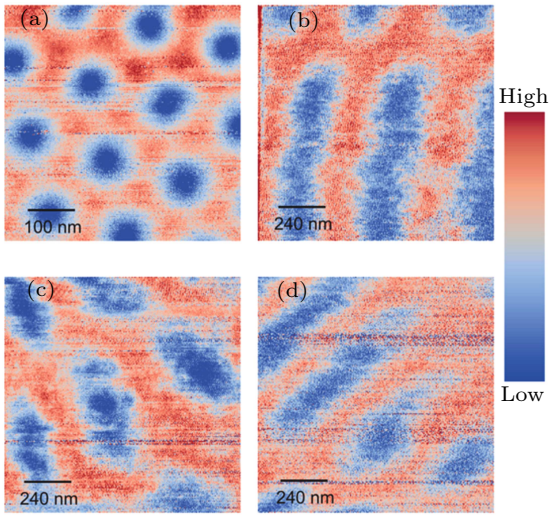


Fig. 1. Characterization manipulation of a vortex lattice on $NbSe_2$ using STM with different tip materials. (a) Characterization of a stationary vortex lattice using a tungsten (W) tip. (b)–(d) Characterization of a moving vortex lattice using a magnetic tip, with tip materials iron (Fe) (b), nickel (Ni) (c) and permalloy (Py) (d). In all $\mathrm{d}I/\mathrm{d}V$ maps in this paper, blue refers to the vortex.

Figures 1(b)–1(d) show vortex movement experiments using strong magnetic tips including hard magnetic Fe (Fig. 1(b)) and Ni tips (Fig. 1(c)), and a soft magnetic Py tip (Fig. 1(d)). The tip's magnetization process was controlled by polarizing the tip in a 70 G field for one minute to minimize the effect of its remanent magnetization. After polarization, the magnetic field was removed. We found that the remanent magnetization of the tip itself is already high enough to generate (and manipulate) vortex lattice.

The striped vortex patterns in Figs. 1(b)–1(d) demonstrate collective vortex motion driven by the remanent stray magnetic field of the tip during scanning. We found that the vortex lattices have ~ 500 nm spacing, corresponding to a remanent field of ~ 100 G, similar to the vortex lattice generated by the Ni tip in a previous STM experiment.[32] The striped patterns exhibit a significant increase in both length (several hundred nm) and width (several tens of nm) of the vortex array. In the fast-scanning direction, the vortices are pulled back and forth by the tip during forward and backward scans, resulting in displacements of several tens of nm. In the slow-scanning direction, the tip couples with the vortex on each scan line, progressively pulling it in the slow direction and forming a striped pattern.

4. Discussion

We confirmed the vortex movement by analyzing its displacement during the scanning process with the magnetic tip. In the STM setup, the tip scans in the forward (FWD) direction and then reverses to scan backward (BWD), generating corresponding FWD and BWD images. By comparing the $\mathrm{d}I/\mathrm{d}V$ maps from both scans, we observe that the vortex positions in

the FWD and BWD scans do not overlap, indicating the tip's interaction with and displacement of the vortex. In the fast-scanning direction, a displacement of approximately 50 nm occurs, while in the slow-scanning direction, the vortices form continuous long stripes (Fig. 2(a)). The characterization and movement of the vortex depend on the distance between the magnetic tip and the vortex during scanning. The tip must be positioned directly above the vortex to characterize it, while due to the long-range nature of the magnetic force, it can still exert a traction force even at greater distances. This attractive force, arising from the same polarity between the tip and vortices generated by the tip's residual magnetism, decreases with increasing distance.[33] Since the tip scans much faster than the vortex can respond, the duration of their interaction determines how far the vortex moves, making scanning speed a key factor in vortex displacement.

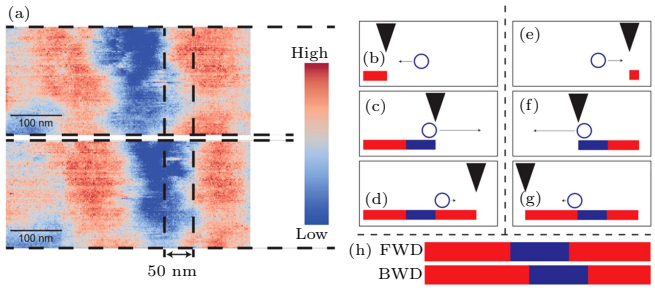


Fig. 2. Analysis of vortex movement induced by a magnetic tip. (a) Simultaneous forward (FWD) (upper panel) and backward (BWD) (lower panel) STM images of a moving vortex lattice characterized using an Fe tip. (b)–(g) Position and force relationship between the tip and a specific vortex. (b)–(d) Correspond to the FWD process: tip moves toward the vortex (b), tip is above the vortex (c), tip moves away from the vortex (d). (e), (g) Correspond to the BWD process: tip returns toward the vortex (e), tip is above the vortex (f), tip moves away from the vortex (g). (h) Simulation of the vortex trace recorded by the tip.

We illustrate our analysis in Figs. 2(b)–2(g). In the fast-scanning direction, the tip starts from the left, increasing its traction on the vortex as it approaches, pulling the vortex slightly to the left (Fig. 2(b)). As the tip moves across the vortex, it causes the vortex to oscillate back and forth (Fig. 2(c)). Once the tip moves past the vortex, the traction decreases, pulling the vortex to the right (Fig. 2(d)). When the tip reverses direction, the traction force increases again, pulling the vortex to the right (Fig. 2(e)) and causing similar oscillations (Figs. 2(f) and 2(g)). As the tip continues scanning, the vortex moves back and forth, forming a wider pattern. The BWD pattern is displaced approximately 50 nm to the right relative to FWD pattern, corresponding to the maximum displacement at the given scanning speed (Fig. 2(h)). After each scan, the vortex's horizontal position in the fast-scanning direction remains roughly the same, while in the slow-scanning direction, it moves continuously, forming a long-stripe pattern. Quantitatively, in some datasets, the stripe lengths in the slow direction range from tens of nm to 1 μm, influenced by factors such as surface flatness and scanning speed.

After confirming that the hard magnetic tip can move the vortex lattice, we tested its long-range motion by adjusting the tip's scanning direction to better control vortex dynamics. It turns out that the vortex moves in a fixed direction by a hard magnetic tip, while the vortex can move with the scanning direction by a soft magnetic tip. Namely, by using an Fe tip, vortex motion consistently occurs in a specific direction, as displayed in Fig. 3(a). This behavior is due to the large remanence and strong in-plane anisotropy of the tip material. As verification, vortex movement along a different single direction after reorienting the tip confirmed that the vortex moves along the main magnetization direction, aligning with the tip's maximum in-plane remanence. In contrast, the soft magnetic FeSiB tip allows the vortex to move in any direction along the slow scanning axis due to its weak remanence and minimal anisotropy. By rotating the scanning direction in 90° increments, we could rotate the vortex array in place, with each movement spanning approximately 300 nm, as shown in Fig. 3(b), which highlights a change in a specific vortex's direction, demonstrating collective, directional movement of the vortex array.

To better control the vortex, enabling switching between static and dynamic vortex lattice motion, and to manipulate a single vortex, it is crucial to regulate the magnetization of the magnetic tip. Initially, the tip's magnetization is roughly adjusted to demagnetize it, ensuring that the tip and the vortex are independent. Fine-tuning the tip's magnetization subsequently modifies its stray field, enabling control over the traction force on the vortex and achieving static-dynamic switching. Following this strategy, a solenoid device, consisting of an FeSiB tip surrounded by a copper-enameled coil, is introduced into the MSTM system (Figs. 4(a) and 4(b)). The demagnetization capacity is tested through a saturation polarization experiment, in which an FeSiB tip is first saturated by a 500 G field, followed by the removal of the polarizing field (Fig. 4(c)). The current in the copper-enameled coil (I_{cec}) is gradually adjusted, altering the tip's magnetization (Fig. 4(c)), followed by vortex mapping at each change of I_{cec} to determine the tip's magnetization (Figs. 4(d)–4(g)), calculated from the measured vortex lattice spacing. The I_{cec} also heats the sample, eventually decreasing the vortex resolution. When $I_{\mathrm{cec}} = 20$ mA, the temperature increases to the point where the vortex is almost indistinguishable (Fig. 4(f)). A reverse I_{cec} experiment confirms the coil's ability to demagnetize the tip, with an adjustable range up to 100 G (Fig. 4(c)). These results demonstrate effective regulation of the magnetic tip, enabling improved manipulation of single vortices.

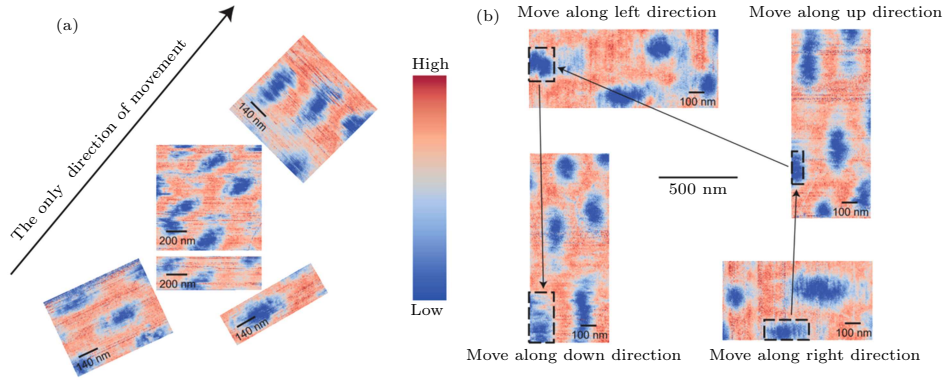


Fig. 3. Vortex lattice movement along a single or arbitrary direction induced by hard or soft magnetic tips. (a) Vortex lattice movement in a single direction induced by hard magnetic Fe tip. (b) Vortex lattice movement in a circle induced by the soft magnetic FeSiB tip.

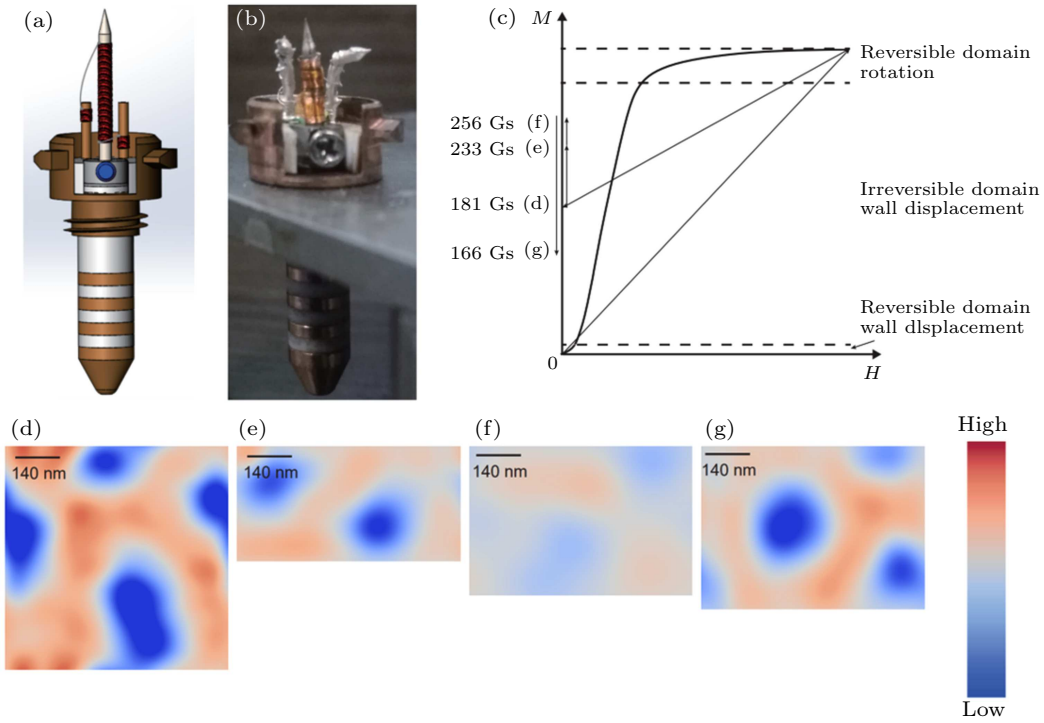


Fig. 4. Vortex lattice manipulated by a magnetism-tunable FeSiB tip using a solenoid device. Design drawing (a) and physical image (b) of the solenoid device. (c) Schematic diagram of the magnetization curve for soft magnetic materials like FeSiB. (d)–(g) Vortex lattice behavior under different tip magnetism tuned using a solenoid device. Coil current is $I = 0$ mA (d), $I = 10$ mA (e), $I = 20$ mA (f), and $I = -5$ mA (g). The effective magnetic field M, calculated from experimental vortex lattice constant, is marked by the corresponding letter in (c).

5. Summary

We employed a strong magnetic tip to induce the overall motion of the vortex array, generated by the tip's remanent magnetic field. This was validated through staged analysis of the tip–vortex relationship, based on vortex movement data from FWD and BWD images. Additionally, we employed a soft magnetic tip to manipulate the vortex array's motion in any direction, effectively simulating the basic operations required for vortex braiding. To enhance control over a single vortex, we developed a strong magnetic tip demagnetization technique based on MSTM. The solenoid device demonstrated effective demagnetization, providing a solid foundation for decoupling the vortex from the tip, followed by control over static and dynamic vortex switching and ultimately enabling the manipulation of a single vortex.

Acknowledgements

Project supported by the National Key Research & Development Program of China (Grant Nos. 2019YFA0308600 and 2020YFA0309000), the National Natural Science Foundation of China (Grant Nos. 92365302, 92065201, 22325203, 92265105, 12074247, 12174252, and 52102336), the Strategic Priority Research Program of Chinese Academy of Sciences (Grant No. XDB28000000), and the Science and Technology Commission of Shanghai Municipality (Grant Nos. 2019SHZDZX01, 19JC1412701, 20QA1405100, 24LZ1401000, and LZPY2024-04). We also acknowledge financial support from the Innovation Program for Quantum

Science and Technology (Grant No. 2021ZD0302500).

References

[1] Binnig G and Rohrer H 1987 *Rev. Mod. Phys.* **59** 615
[2] Hofer W A, Foster A S and Shluger A L 2003 *Rev. Mod. Phys.* **75** 1287
[3] Wiesendanger R 2009 *Rev. Mod. Phys.* **81** 1495
[4] Oka H, Brovko O O, Corbetta M, Stepanyuk V S, Sander D and Kirschner J 2004 *Rev. Mod. Phys.* **86** 1127
[5] Nadj-Perge S, Drozdov I K, Li J, Chen H, Jeon S, Seo J, MacDonald A H, Bernevig B A and Yazdani A 2014 *Science* **346** 602
[6] Xu J P, Wang M X, Liu Z L, Ge J F, Yang X J, Liu C H, Xu Z A, Guan D D, Gao C L, Qian D, Liu L, Wang Q H, Zhang F C, Xue Q K and Jia J F 2015 *Phys. Rev. Lett.* **114** 017001
[7] Sun H H, Zhang K W, Hu L H, Li C, Wang G Y, Ma H Y, Xu Z A, Gao C L, Guan D D, Li Y Y, Liu C H, Qian D, Zhou Y, Fu L, Li S C, Zhang F C and Jia J F 2016 *Phys. Rev. Lett.* **116** 257003
[8] Liu Q, Chen C, Zhang T, Peng R, Yan Y J, Wen C H P, Lou X, Huang Y L, Tian J P, Dong X L, Wang G W, Bao W C, Wang Q H, Yin Z P, Zhao Z X and Feng D L 2018 *Phys. Rev. X* **8** 041056
[9] Wang D F, Kong L Y, Fan P, Chen H, Zhu S Y, Liu W Y, Cao L, Sun Y J, Du S X, Schneeloch J, Zhong R D, Gu G D, Fu L, Ding H and Gao H J 2018 *Science* **362** 333
[10] Zhu Z, Papaj M, Nie X A, Xu H K, Gu Y S, Yang X, Guan D D, Wang S Y, Li Y Y, Liu C H, Luo J L, Xu Z A, Zheng H, Fu L and Jia J F 2021 *Science* **374** 1381
[11] Wang M X, Liu C H, Xu J P, Yang F, Miao L, Yao M Y, Gao C L, Shen C Y, Ma X C, Chen X, Xu Z A, Liu Y, Zhang S C, Qian D, Jia J F and Xue Q K 2012 *Science* **336** 52
[12] Xu J P, Liu C H, Wang M X, Ge J F, Liu Z L, Yang X J, Chen Y, Liu Y, Xu Z A, Gao C L, Qian D, Zhang F C and Jia J F 2014 *Phys. Rev. Lett.* **112** 217001
[13] Eigler D M, Lutz C P and Rudge W E 1991 *Nature* **352** 600
[14] Stroscio J A and Eigler D M 1991 *Science* **254** 1319
[15] Whitman L J, Stroscio J A, Dragoset R A and Celotta R J 1991 *Science* **251** 1206
[16] Ge J F, Liu Z L, Gao C L, Qian D, Liu C H and Jia J F 2015 *Rev. Sci. Instrum.* **86** 053903
[17] Duan M C, Liu Z L, Ge J F, Tang Z J, Wang G Y, Wang Z X, Guan D D, Li Y Y, Qian D, Liu C H and Jia J F 2017 *Rev. Sci. Instrum.* **88** 073902
[18] Nayak C, Simon S H, Stern A, Freedman M and Das Sarma S 2008 *Rev. Mod. Phys.* **80** 1083
[19] Elliott S R and Franz M 2015 *Rev. Mod. Phys.* **87** 137
[20] Field B and Simula T 2018 *Quantum Sci. Technol.* **3** 045004
[21] van Heck B, Akhmerov A R, Hassler F, Burrello M and Beenakker C W J 2012 *New J. Phys.* **14** 035019
[22] Polshyn H, Naibert T and Budakian R 2019 *Nano Lett.* **19** 5476
[23] Ma X, Reichhardt C J O and Reichhardt C 2020 *Phys. Rev. B* **101** 024514
[24] Posske T, Chiu C K and Thorwart M 2020 *Phys. Rev. Res.* **2** 023205
[25] Ma H Y, Guan D D, Wang S Y, Li Y Y, Liu C H, Zheng H and Jia J F 2021 *J. Phys. D. Appl. Phys.* **54** 424003
[26] Straver E W J, Hoffman J E, Auslaender O M, Rugar D and Moler K A 2008 *Appl. Phys. Lett.* **93** 172514
[27] Auslaender O M, Luan L, Straver E W J, Hoffman J E, Koshnick N C, Zeldov E, Bonn D A, Liang R X, Hardy W N and Moler K A 2009 *Nat. Phys.* **5** 35
[28] Ge J Y, Gladilin V N, Tempere J, Xue C, Devreese J T, Van de Vondel J, Zhou Y H and Moshchalkov V V 2016 *Nat. Commun.* **7** 13880
[29] Kremen A, Wissberg S, Haham N, Persky E, Frenkel Y and Kalisky B 2016 *Nano Lett.* **16** 1626
[30] Ge J Y, Gladilin V N, Tempere J, Devreese J and Moshchalkov V V 2017 *Nano Lett.* **17** 5003
[31] Wulfhekel W and Kirschner J 1999 *Appl. Phys. Lett.* **75** 1944
[32] Shore J D, Huang M, Dorsey A T and Sethna J P 1989 *Phys. Rev. Lett.* **62** 3089
[33] Roseman M and Grütter P 2002 *Appl. Surf. Sci.* **188** 416